Journal of Environmental Sciences Vol.16, No.1, pp.40—43, 2004

ISSN 1001—0742
CN11—2629/X

Article ID: 1001-0742(2004)01-0040-04 **CLC number**: X131.1 **Document code**: A

Automatic and continuous measurement of aerosol properties in Dunhuang, China

XIA Xiang-ao, WANG Ming-xing, WANG Yue-si

(State Key Laboratory of Atmospheric Boundary Physics and Atmospheric Chemistry, Institute of Atmospheric Physics, Chinese Academy of Sciences, Beijing 100029, China. E-mail: xiangaoxia@sina.com)

Abstract: Ground-based simultaneous observations of sun direct and scattering radiation were carried out in Dunhuang for nearly 2 years. Aerosol optical depth, Angstrom wavelength exponent and size distribution were obtained from solar extinction and sky radiation. Water vapor content was obtained from sun direct radiation measurement at 940 nm. Relationship between aerosol properties and water vapor was discussed. Results showed that distinct seasonality of aerosol optical depth and Angstrom wavelength exponent was corresponding to seasonal variation of dust activity. Aerosol relative size distribution kept stable and volume concentration change was the reason resulting in variation of aerosol optical depth. Water vapor had minor effects on aerosol optical and physical properties.

Keywords: aerosol; aureolemeter; inversion

Introduction

Observations in Barbados suggested that dust aerosol be an important climate forcing agent in source and downwind region(Li, 1996). Globally, three components including sulfate, dust and carbonaceous particles, appeared to contribute equally to the column-integrated total optical depth based on model study (Tegen, 1996a). Comparison between model output with satellite measurements indicated that 50 ± 20% of total atmospheric dust mass originated from disturbed soils(Tegen, 1996b). These findings intrigued more interests in dust radiative forcing since it was not negligible in regional and global scale, furthermore, about half of it was from human unreasonable activities such as cultivation, deforestation, erosion and so on.

Northwest China is the source region of dust aerosol for East Asia. Approximate 800 Tg/a (uncertainty range is 500—1100 Tg/a) (Zhang, 2001) dust aerosols, about half of global dust aerosol emission, are emitted into atmosphere from northwest China owing to frequent occurrence of dust weather, there into, about half is transported to downwind region, so it is of great significance to study dust aerosol effects on atmospheric environment and climate.

Ground-based sunphotometer played an important role in characterizing aerosol properties and determining aerosol effects on local and global climate. So in this paper, we analyzed data continuously collected by advanced aureolemeter in Dunhuang from 1999 to 2000 as a part of Sino-Japan co-operation on dust aerosol.

1 Instrumentation and methodology

The measurements presented in this paper were made in Dunhuang, a famous ancient city with its glorious caves and frescos. Aureolemeter (also called sun/sky radiometer) model pom-01, produced by Prede (Tokyo) was utilized to measure the sky radiance distribution and direct solar irradiance. The following wavelengths (315, 400, 500, 675, 870, 940, 1020 nm) are adopted in measurements by use of the same detector with high dynamic range of 10^7. The first and the sixth wavelengths are for the monitor of ozone absorption optical depth and columnar water vapor content, the others for aerosol. As for filters, except that the half bandwidth is 3 nm for 315 nm wavelengths, the others less than 10 nm. The field of view is 1°, and the minimum angle for sky measurements is about 3°. The photometer is mounted on a vertical-horizontal two-axes mount that is driven by digital servomotors to scan sky radiation distributions. Photometer was calibrated by using of modified Langley method suggested by Nakajima(Nakajima, 1996). The main procedures included: an inversion with only forward scattering intensity data(3°—40°) was performed for all available measurements, and the set of temporarily variable aerosol optical depth, multiplied by the air mass (m), was used to derive values of abscissa for a V-m τ scattering graph, then constant of radiometer was obtained through least square method. Sensitivity study showed that the effects of uncertainties in input parameters such as reflective index, and measurement errors on calibration were weak, so calibration accuracy of 1% can be achieved by this method. Hence, error of aerosol optical depth measurement was approximate 0.01 at one air mass. Surface pressure needed for Rayleigh scattering optical depth calculation was from Dunhuang meteorological observatory; columnar ozone content for ozone absorption optical depth calculation was from TOMS data, both of these two optical depths were required to be subtracted from total optical depth measurement to get aerosol information. Total column water vapor was retrieved primarily from direct sun measurements at the wavelength of 940 nm based on the technique of Bruegge *et al*. (Zhu, 1998). Cloud screening method developed by Smirnov *et al*. (Smirnov, 2000) was utilized in data quality verification. This technique relies on principle that cloud has larger optical depth and greater temporal variance compared to aerosol. Angstrom wavelength exponent, which is a measure of the wavelength dependence of aerosol optical depth and therefore sensitive to particle size distribution, was calculated from linear regression of optical depth and wavelength in logarithmic space. Aerosol size distributions were retrieved by procedure called SKYRAD that was developed by Nakajima (Nakajima, 1996). The code consists of two parts; the first is improved multiple scattering radiative transfer scheme in a plane-parallel atmosphere developed by Nakajima, and the second part is constrained linear inversion scheme. Its inversion accuracy was discussed in detail in the literature(Nakajima, 1996; Tonna, 1995). On the average, the

Foundation item: The National Natural Science Foundation of China(No. 40175008); * Corresponding author

errors for the two ends(0.05—0.1 and 7—15) may be as large as 35%—100%, but the precision for middle range is expected to be about 20%.

2 Results and discussion

2.1 Aerosol optical depth and Angstrom wavelength exponent

Fig.1a showed the monthly average of aerosol optical depth at 500 nm for 2 years, with error bars depicting one standard deviation of the daily average values. Monthly variation of Angstrom wavelength exponent is shown in Fig.1b. Larger aerosol optical depth and smaller exponent appeared in spring, corresponding to higher probability of occurrence of dust weather in this season, furthermore, on the average, larger optical depth was companied by larger deviation, it was not surprising because greater difference in aerosol concentration existed between dust activity and normal period. Autumn is the cleanest season in Dunhuang with small aerosol optical depth and relatively larger Angstrom parameter. Fig. 2 shows the diurnal variation of optical depth and Angstrom wavelength exponent for 12 months. There were no large differences among all months, basically, diurnal distribution with uni-peak was the feature for all months and peak appeared at local time 3:00 to 4:00, meaning higher probability of dust activity, which was accordance with surface observations (Niu, 2000). This feature may bear relation to strong solar irradiance and resulted strong turbulence and convection that is in favor of dust activity and transportation during this period. In addition, late morning average (10:00—11:30 local time) represent 90% of the entire daily average values, on the contrary, early afternoon (12:30—14:00 local time) averages exceeded the entire daily average values with 10%—15%. Satellite, such as Terra and Aqua, collected data during these two periods, so combination of two satellite measurements should represent daily average better.

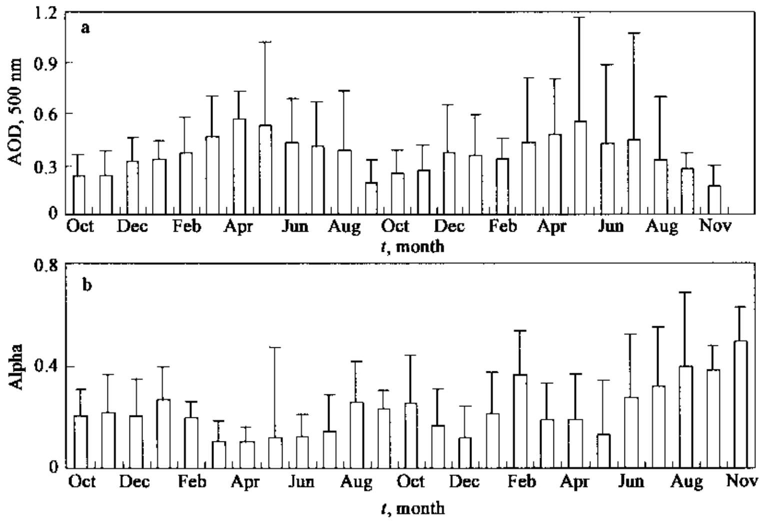

Fig.1 Monthly average of aerosol optical depth(500 nm)
a. Angstrom parameter(ALPHA); b. the error bars describe one standard deviation

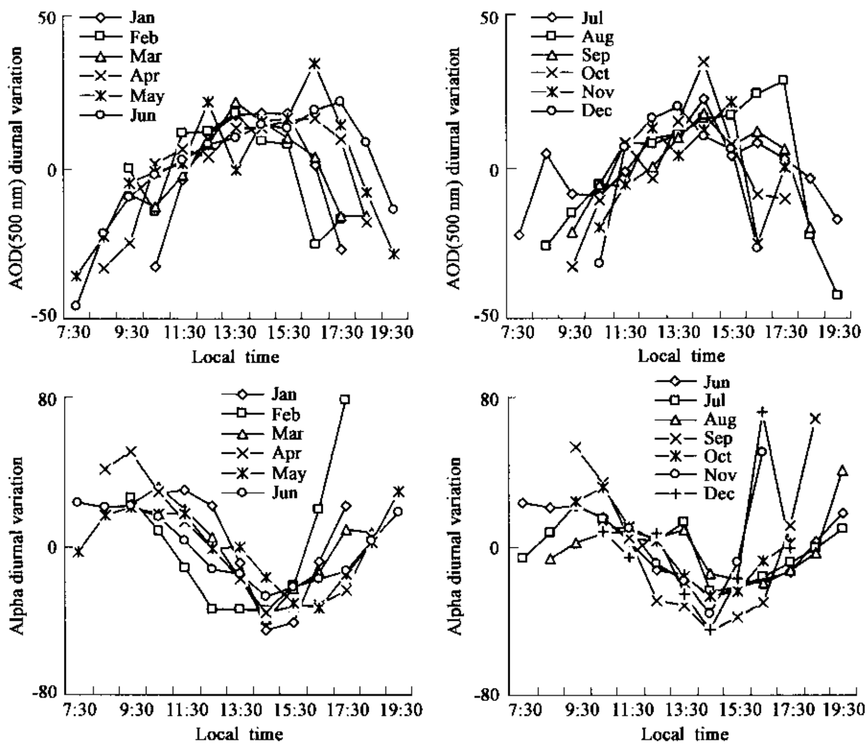

Fig.2 Diurnal variation of aerosol optical depth(500 nm)(left) and Angstrom parameter(ALPHA) (right) for twelve months

2.2 Aerosol size distribution

The retrieved aerosol volume size distributions for aerosol optical depth at 500 nm varying from 0.08 to 0.97 are shown in Fig.3. Aerosol size distribution retrievals were derived from simultaneous analysis of sky radiances and spectral optical depth at five wavelengths. Each size distribution in Fig. 3 was the average computed from at least 40 individual retrievals. Sky radiances in inversion was limited to forward scattering direction(3°—40°), the reason was that non-spherical effects of dust aerosol on inversions was negligible in these regions. As seen in Fig.3, size distribution in Dunhuang may be characterized by the sum of two log normals as follows:

$$v(r) = \frac{dV(r)}{d\ln r} = \sum_{i=1}^{2} \frac{C_{V,i}}{\sigma_i} \exp\left[- \frac{(\ln r - \ln r_{r,i})^2}{2\sigma_i^2} \right].$$

Where $r_{r,i}$ is the volume median radius, σ_i is the standard deviation, $C_{V,i}$ is the volume concentration for accumulation and coarse mode. Obviously, the coarse mode particles dominate over accumulation, which is the distinguished character of dust aerosol in source region. There was no tendency for increasing particle volume median radius as aerosol optical depth increases, but only increase of particle concentration, which was evident in linear regression analysis between aerosol optical depth with volume median radius and standard deviation for two modes, the results showed no significant relations existed, but volume concentration of two modes had statistically significant positive relation with aerosol optical depth (r^2 is 0.75 and 0.78, individually). This character was different from smoke and urban aerosols. Significantly positive relation between volume median radius for accumulation mode and optical depth existed for these two aerosol types (Remer, 1998; Eck, 2001).

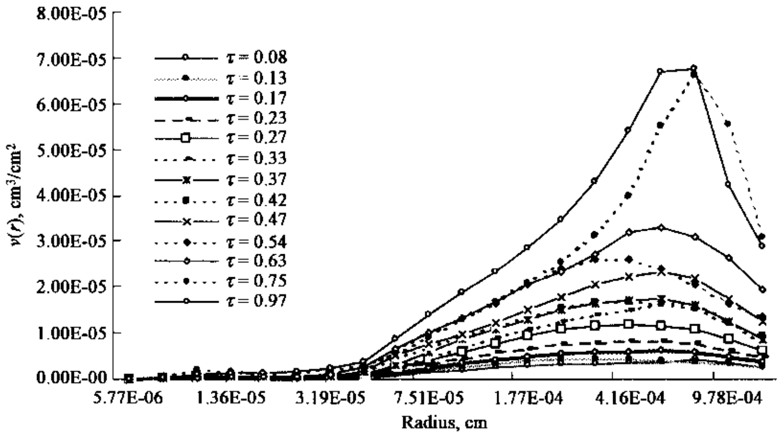

Fig.3 Aerosol volume size distribution for aerosol optical depth at 500 nm varying from 0.08 to 0.97. Each aerosol size distribution is an average of about 40 retrievals derived from solar direct and scattering radiation at 400, 500, 675, 870, 1020 nm. Sky radiance is limited to 3°—40°

2.3 Aerosol properties and water vapor

Fig.4 shows the relation between aerosol properties and water vapor for total daily average value. Evidently, there is no statistically significant relation between water vapor and optical depth, and Angstrom exponent. The same results were obtained when analyses were carried out based on seasonal data. These results demonstrated that humidification capability of dust aerosol in Dunhuang was weak, in addition, it might indicate that no distinct difference in water vapor content was in existence between dusty and normal days, which was also different from smoke and urban aerosols with higher humidification capability.

3 Conclusions

Simultaneous measurements of solar direct and scattering radiation were made in Dunhuang for nearly two years. Based on careful calibration and inversion, we can make some conclusions as follows:

Distinct seasonal variation appeared in optical depth and Angstrom wavelength exponent corresponding to seasonal dust activity. Spring had the largest optical depth and the smallest exponent, and larger exponent and smaller optical depth appeared in autumn. Coarse mode dominated over cumulative in Dunhuang. The variation of aerosol optical depth was mainly resulted from change of volume concentration for cumulative and coarse mode, but size parameters for cumulative and coarse did not change. Water vapor had weak influence on dust optical and physical properties because of dust aerosol low humidification capability, which was different from other types.

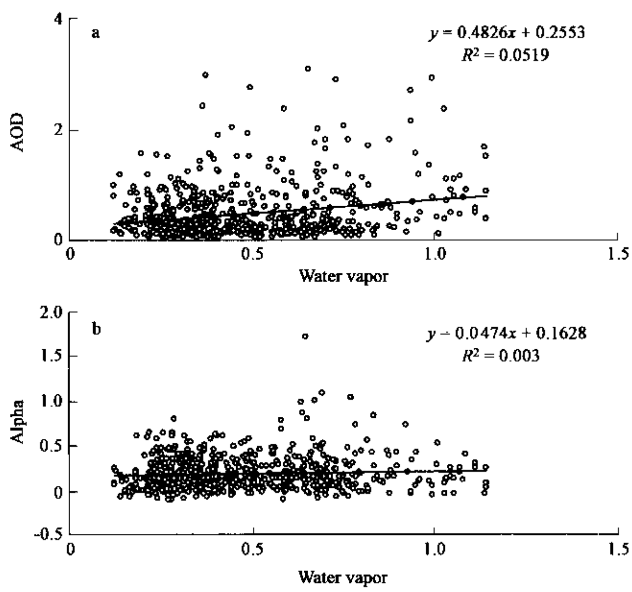

Fig.4 Scattering plot between water vapor content with aerosol optical depth (500 nm)(a) and Angstrom parameter(alpha)(b), also shown are equations and interpretation standard deviations for linear regression analysis

References:

Eck T F, Holben B N, Dubovik O *et al*., 2001. Column integrated aerosol optical properties over the Maldives during the northeast monsoon for 1998—2000[J]. J Geophys Res, 106: 28555—28566.

Li X H M, Savoie D, Voss K *et al*., 1996. Dominance of mineral dust in aerosol light-scattering in the North Atlantic trade winds[J]. Nature, 380: 416—419.

Nakajima T, Tonna T, Rao R *et al*., 1996. Use of sky brightness measurements from ground for remote sensing of particulate polydispersions[J]. Appl Opt, 35: 2672—2686.

Niu S J, Sun J, Sang J, 2000. Trend of sandstorm occurrence in Helan Moutain area[J]. J Desert Res, 20: 55—58.

Remer L A, Kaufman Y J, 1998. Dynamic aerosol model: urban/industrial aerosol [J]. J Geophys Res, 1998: 31879—31891.

Smirnov A, Holben B N, Slutsker I *et al*., 2000. Cloud screening and quality control algorithms for the AERONET data base[J]. Remote Sens Environ, 73: 337—349.

Tegen I, Hollrig P, Chin M *et al*., 1996a. Contribution of different aerosol species to the global aerosol extinction optical thickness: estimates from model results[J]. J Geophys Res, 102: 23895—23915.

Tegen I, Lacis A A, Fung I, 1996b. The influence on climate forcing of mineral aerosols from disturbed soils[J]. Nature, 380: 419—422.

Tonna G, Nakajima N, Rao R *et al*., 1995. Aerosol features retrieved from solar aureole data: a simulation study concerning a turbid atmosphere[J]. Appl Opt, 34: 4486—4499.

Zhang X Y, 2001. Source, distribution, emission, transport, deposition of Asia dust and loess accumulation[J]. Quaternary Sciences, 21: 39—40.

Zhu X S, Zhou J, 1998. Determination of clear-sky columnar water vapor using solar radiometer[J]. Chinese J Atmos Sci, 22: 39—45.

(Received for review September 23, 2002. Accepted January 7, 2003)